AIAA Atmospheric Flight Mechanics Conference
08 - 11 August 2011, Portland, Oregon

AIAA 2011-6356

Validating the Multidimensional Spline Based Global Aerodynamic Model for the Cessna Citation II

C.C. de Visser,* J.A. Mulder,†
Q.P. Chu‡
Delft University of Technology, Delft, The Netherlands

The validation of aerodynamic models created using flight test data is a time consuming and often costly process. In this paper a new method for the validation of global nonlinear aerodynamic models based on multivariate simplex splines is presented. This new method uses the unique properties of the multivariate simplex splines, a recent type of of multivariate spline, to speedup the process of aerodynamic model validation. Multivariate simplex splines are defined on non-rectangular domains and can be used to accurately fit scattered nonlinear datasets in any number of dimensions. The simplex splines consist of piecewise defined, ordinary multivariate polynomials with a predefined continuity between neighboring polynomial pieces. A recent method for nonlinear system identification based on multivariate simplex splines was used to create a global nonlinear aerodynamic model of the Cessna Citation II laboratory aircraft operated by the Delft University of Technology. In this paper, the multivariate spline based aerodynamic model for the pitching moment coefficient will be validated using both a model residual analysis as well as a statistical model quality analysis. It will be demonstrated that these new analysis methods, which are both unique to the multivariate simplex splines, provide a highly efficient and powerful new method for aerodynamic model validation.

Nomenclature

$\bar{c}$ = mean aerodynamic chord, m
$\hat{d}$ = total number of polynomial terms in basis function
$\mathbf{B}$ = global data location matrix
$\mathbf{c}$ = global B-coefficient vector
$\mathbf{D}$ = global data sifting matrix
$\mathbf{H}$ = smoothness matrix
$\mathbf{I}$ = inertia matrix, $kg \cdot m^2$
$\mathbf{X}$ = regression matrix
$\mathbf{Y}$ = measurement vector
$\mathcal{T}$ = triangulation formed by a set of simplices
A_x, A_y, A_z = specific forces along body $X/Y/Z$ axis, m/s^2
a_x, a_y, a_z = kinematic accelerations along body $X/Y/Z$ axis, m/s^2
b = barycentric coordinate
$B^d_\kappa(b)$ = individual polynomial basis function term of degree d
C = general dimensionless coefficient,-
c_κ = individual B-coefficient

*Ph.D. student, Control and Simulation Division, Faculty of Aerospace Engineering, P.O. Box 5058, 2600GB Delft, The Netherlands; c.c.devisser@tudelft.nl. Student member AIAA.
†Professor, Control and Simulation Division, Faculty of Aerospace Engineering, P.O. Box 5058, 2600GB Delft, The Netherlands; j.a.mulder@tudelft.nl. Member AIAA.
‡Associate Professor, Control and Simulation Division, Faculty of Aerospace Engineering, P.O. Box 5058, 2600GB Delft, The Netherlands; Q.P.Chu@tudelft.nl. Member AIAA.

d = polynomial degree
g = gravity constant, m/s^2
L, M, N = combined aerodynamic and thrust moments about the body $X/Y/Z$ axis, $N \cdot m$
m = mass, kg
n = spline dimension
$p(b)$ = general polynomial in barycentric coordinates
p, q, r = roll, pitch, and yaw rates around the body $X/Y/Z$ axis, rad/s
r = continuity order of spline function
S = wing area, m^2
S_d^r = spline space of degree d and continuity order r
T_c = dimensionless thrust, -
t_i = single simplex
u_b, v_b, w_b = airspeed velocity components along body $X/Y/Z$ axis, m/s
u_e, v_e, w_e = airspeed velocity components along Earth's fixed $X/Y/Z$ axis, m/s
V = airspeed, m/s
X, Y, Z = combined aerodynamic and thrust forces along the body $X/Y/Z$ axis, N
x, y, z = position coordinates along $X/Y/Z$ axis, m (reference frame varies)

Symbols

α, β, γ = angle of attack, angle of sideslip, and flightpath angle, rad
δ = control surface deflection, rad (subscript determines specific control surface)
κ = multi-index
λ = bias
ϕ, θ, ψ = roll, pitchm and yaw angles, rad
ρ = air density, kg/m^3

Subscripts

κ = multi-indexed entity
a, e, r = aileron, elevator and rudder
$c.g.$ = center of gravity
i, j = general indexers
l, m, n = combined aerodynamic and thrust moment about the body $X/Y/Z$ axis, $N \cdot m$
sp = spoiler
tr = trim tab

Superscripts

a, e, r = aileron, elevator and rudder
$c.g.$ = center of gravity
l, m, n = combined aerodynamic and thrust moment about the body $X/Y/Z$ axis, $N \cdot m$
sp = spoiler
t_i = simplex identifier

I. Introduction

High quality aerodynamic models are essential in the adequate functioning of flight simulators and flight control systems. Identifying and validating aerodynamic models using flight test data is a costly and often time consuming task. Currently, the most widely used method for identifying aerodynamic models uses a parameter estimation method like least squares or maximum likelihood to estimate the parameters of a polynomial regression model.[1,2,3,4,5,6,7,8,9] More complex models can be created by identifying local polynomial models on sub-partitions of the flight envelope. The set of local polynomial models can then be blended into a single smooth structure using fuzzy blending techniques or neural networks.[10] However, these blending methods suffer from a number of important drawbacks such as loss of transparency, loss of the linear-in-the-parameter property of the polynomial models and the arbitrariness of the blending operation.

Many authors have therefore suggested the use of polynomial spline functions for fitting flight data.[11,12,8] Spline functions are piecewise defined polynomials with a predefined continuity order between pieces. The approximation power of spline functions is proportional with the degree of the polynomial but also with the number and density of the polynomial pieces. Polynomial spline functions are capable of fitting highly nonlinear datasets over large domains. While one-dimensional, or (i.e. univariate) spline theory is well known and developed, multi-dimensional (i.e. multivariate) spline theory is still an active research field. Many different multivariate spline types exist, such as the DMS-spline[13] and the well known and much used tensor product B-spline.[14] Multivariate tensor product splines have been successfully used in the past to model aircraft aerodynamics. Smith,[11] Klein[4] and Bruce[12] used bivariate tensor product splines in a linear regression framework for the purpose of aerodynamic model identification. Tensor product splines, however, have a number of fundamental drawbacks. They are defined exclusively on rectangular domains which greatly limits their flexibility. More importantly, it is well known that the multivariate tensor product spline is for fundamental mathematical reasons incapable of fitting scattered data.[15] This makes the tensor product spline useless for the fitting of flight test data, which is inherently scattered.

Recently, a new type of multivariate spline for scattered data approximation was introduced.[16] Called the multivariate simplex spline, it is capable of fitting nonlinear, multi-dimensional scattered data[16,17,18] and has an arbitrarily high approximation power. Simplex splines are not defined on rectangular domains and are therefore much more flexible than tensor product splines. Recently, a linear regression framework for multivariate simplex splines was introduced[18] which allows the use of standard parameter estimation techniques such as Least Squares (LS) or Maximum Likelihood (ML) for estimating the parameters of the simplex spline polynomials. A significant advantage of the new identification method over other methods is that polynomial structure selection is performed during the parameter estimation step, rather than in a separate polynomial model structure selection step like in the state of the art method presented by Lombaerts et al. in.[19] Instead of selecting individual polynomial terms beforehand, all polynomial terms of total degree d are considered during parameter estimation. This is possible because the local basis functions of the simplex splines are members of the complete space of polynomials of degree d.

Fig. 1 Cessna Citation II laboratory aircraft

In two recent papers, the authors demonstrated a new method for aerodynamic model identification based on multivariate simplex splines. In[20] a global aerodynamic model based on multivariate simplex splines for the F-16 fighter aircraft was created. This spline model was based on simulated flight test data from a public domain NASA subsonic wind tunnel model of the F-16. In[21] a multivariate spline based global aerodynamic model for the Cessna Citation II laboratory aircraft (PH-LAB) was created. This model is based on flight data obtained during 76 flight test manoeuvres, and is used in the demonstration of the new model validation method.

The objective of this paper is the demonstration of a new method for validating aerodynamic models based on multivariate simplex splines. The multivariate simplex splines have a number of unique properties that enable two new approaches to model quality analysis. The first new approach in model quality analysis is a model residual analysis, which results in a new multivariate spline function for empirical model confidence bounds. The second new approach is a statistical model quality analysis which results in a Cramér-Rao Lower Bound (CRLB) parameter hyper-surface. This is possible because the parameters of the multivariate simplex spline each have a unique spatial location within the model domain, which means that their respective variances and CRLB's are bound to that same spatial location.

The new model validation method was demonstrated on the multivariate simplex spline based model for the aerodynamic pitching moment coefficient of the Cessna Citation II. The two new model quality analysis methods clearly show that the quality of this model varies strongly across the flight envelope. While the quality of the model is shown to be very high in the central regions of the flight envelope, regions closer to the model domain boundaries have a significantly lower quality.

II. Preliminary on Multivariate Simplex Splines

In this section a brief introduction is given on the basic theory of multivariate simplex splines. For an excellent in-depth coverage of the matter we would like to refer to the work of Lai and Schumaker.[22]

A. The Simplex and Barycentric Coordinates

The individual spline pieces of the simplex spline are defined on simplices. A simplex is a geometric structure that provides a minimal, non-degenerate span of n-dimensional space. For example, the simplex of 2-dimensional space is the triangle and the simplex of 3-dimensional space the tetrahedron. Note that in the following we use 'n-simplex' as shorthand for 'the simplex of n-dimensional space'. A simplex is defined as follows. Let V be a set of $n+1$ unique, non-degenerate, points in n-dimensional space:

$$V := \{v_0, v_1, \dots, v_n\} \in \mathbb{R}^n \tag{1}$$

Then the convex hull of V is the n-simplex t:

$$t := \langle V \rangle \tag{2}$$

The boundary edges of a simplex are called *facets*. A facet of an n-simplex is a $(n-1)$-simplex by definition; it is constructed from all but one of the vertices of the n-simplex.

The simplex has its own local coordinate system in the form of the barycentric coordinate system. The barycentric coordinate system is instrumental in the definition of the stable local polynomial basis for the multivariate spline. The principle of barycentric coordinates is the following; every point $x = (x_1, x_2, \dots, x_n)$ inside or outside the convex hull of a simplex t, with t as in Eq. (2), can be described in terms of a unique weighted vector sum of the vertices of t. The barycentric coordinate $b(x) = (b_0, b_1, \dots, b_n)$ of x with respect to simplex t are these vertex weights:

$$x = \sum_{i=0}^{n} b_i v_i \tag{3}$$

The barycentric coordinates are normalized, i.e.

$$\sum_{i=0}^{n} b_i = 1 \tag{4}$$

B. Triangulations of Simplices

A triangulation $\mathcal{T}$ is a special partitioning of a domain into a set of J non-overlapping simplices.

$$\mathcal{T} := \bigcup \{t_i,\ i = 0, 1, \dots, J\} \tag{5}$$

In a valid triangulation simplices are not allowed inside the convex hull of other simplices:

$$t_i \cap t_j \in \left\{\emptyset, \tilde{t}\right\}, \quad \forall t_i, t_j \in \mathcal{T} \tag{6}$$

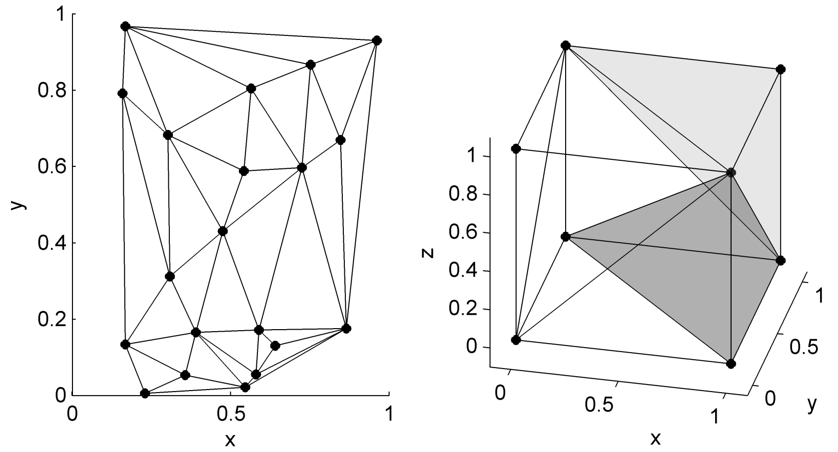

Fig. 2 2-D Delaunay triangulation consisting of 31 triangles (left) and 3-D Delaunay triangulation consisting of 6 tetrahedrons (right, two tetrahedrons are colored for clarity).

with $\tilde{t}$ a k-simplex with $0 \leq k \leq n-1$.

One of the most common triangulation methods is the Delaunay triangulation. Fig. 2 shows two Delaunay triangulations. In the left hand plot the Delaunay triangulation of 20 randomly distributed vertices in 2-D is shown. This triangulation consists of 31 triangles. In the right hand plot the Delaunay triangulation of 8 uniformly distributed vertices in 3-D is shown. This triangulation consists of 6 tetrahedrons. It should be noted at this point, that creating a triangulation using the Delaunay algorithm does not always result in a well-defined triangulation, as has been pointed out in the literature.[23] It is possible that so-called *sliver* simplices are produced, which are simplices which have a very large circum (hyper) sphere compared to their size.[23] Polynomials defined on sliver simplices tend to be badly conditioned possibly leading to numerical instability, so their creation should be avoided as much as possible.

For our applications, we have developed a simple but powerful method for creating well defined triangulations suitable for use in aerodynamic model identification. This method does not use the Delaunay triangulation method, but instead fits a predefined number of (hyper) cubes inside the convex hull of a given dataset. The hypercubes themselves are then triangulated individually, resulting in a well defined triangulation such as that demonstrated in Fig. 3.

C. Spline Spaces

A spline space is the space of all spline functions s of a given degree d and continuity order C^r on a given triangulation $\mathcal{T}$. Such spline spaces have been studied extensively, see e.g.[24,25,22] We use the definition of the spline space from:[22]

$$S_d^r(\mathcal{T}) := \{s \in C^r(\mathcal{T}) : s|_t \in \mathbb{P}_d, \ \forall t \in \mathcal{T}\} \tag{7}$$

with $\mathbb{P}_d$ the space of all polynomials of total degree d. The definition of the spline space in Eq. (7) provides a convenient notation for stating the degree, continuity and triangulation of a spline solution without having to specify individual spline functions. For example, $S_3^1(\mathcal{T})$ is the space of all cubic spline functions with continuity order C^1 defined on the triangulation $\mathcal{T}$.

D. The B-form of the multivariate simplex spline

The polynomials of the simplex spline can be expressed in the so-called B-form. The B-form provides an elegant notation for the linear combination of Bernstein basis functions on a single n-simplex. In the following, we will provide a derivation of the B-form of the multivariate simplex spline. Starting with the definition of the multinomial theorem, we have:

$$(b_0 + b_1 + \cdots + b_n)^d = \sum_{\kappa_0+\kappa_1+\cdots+\kappa_n=d} \frac{d!}{\kappa_0!\kappa_1!\cdots\kappa_n!} \prod_{i=0}^{n} b_i^{\kappa_i}. \tag{8}$$

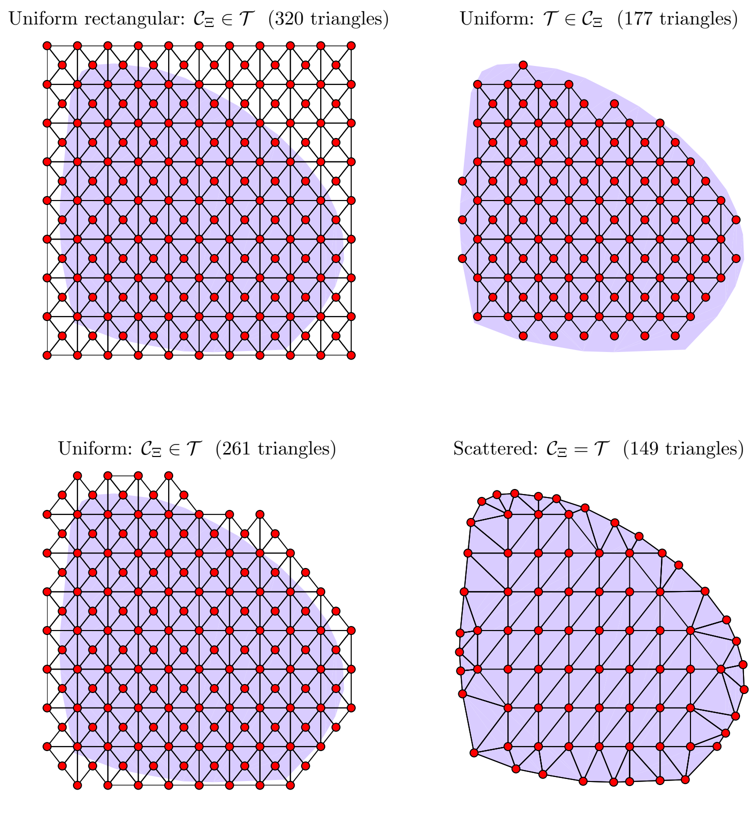

Fig. 3 Four different methods of triangulating a data domain (shaded area). Top left: a uniform rectangular triangulation; top right: an underfitted uniform triangulation; bottom left: a overfitted uniform triangulation; bottom right: an exact fit scattered triangulation

Now let the multi-index κ be defined as follows:

$$\kappa := (\kappa_0, \kappa_1, \ldots, \kappa_n) \in \mathbb{N}^{n+1}. \tag{9}$$

The 1-norm of the multi-index is given by:

$$|\kappa| = \kappa_0 + \kappa_1 + \cdots + \kappa_n = d, \quad d \geq 0. \tag{10}$$

The multi-index provides a convenient mechanism for covering all possible integer permutations that sum up to a value d.

□ **Example:** List all valid permutations of κ for $|\kappa| = 2$ and $n = 2$. For $n = 2$ we have $\kappa = (\kappa_0, \kappa_1, \kappa_2)$. The set of valid permutations of κ are:

$$\kappa \in \{(2,0,0),(1,1,0),(1,0,1),(0,2,0),(0,1,1),(0,0,2)\}.$$

□

Hu[26] and Lai[22] introduce a very useful *lexicographical* sorting order on the elements of the multi-index:

$$\kappa_{d,0,0\cdots0} > \kappa_{d-1,1,0\cdots0} > \kappa_{d-1,0,1,0\cdots0} > \cdots > \kappa_{0\cdots0,1,d-1} > \kappa_{0\cdots0,0,d}. \tag{11}$$

The total number of valid permutations of κ is $\hat{d}$:

$$\hat{d} = \frac{(d+n)!}{n!d!}. \tag{12}$$

Using the multi-index from Eq. (9) the multinomial equation Eq. (8) can be simplified into:

$$(b_0 + b_1 + \cdots + b_n)^d = \sum_{|\kappa|=d} \frac{d!}{\kappa!} b^\kappa. \tag{13}$$

□ **Example:** Expand the multinomial expression for $n = 2$ and $d = 2$ using the multi-index κ.
In this case we have $\kappa = (\kappa_0, \kappa_1, \kappa_2)$ with permutations $\kappa \in \{(2,0,0),(1,1,0),(1,0,1),(0,2,0),(0,1,1),(0,0,2)\}$.
The multinomial equation Eq. (13) then is:

$$\begin{aligned}
(b_0 + b_1 + b_2)^2 &= \sum_{|\kappa|=2} \frac{2!}{\kappa!} b^\kappa \\
&= \frac{2!}{2!0!0!} b_0^2 b_1^0 b_2^0 + \frac{2!}{1!1!0!} b_0^1 b_1^1 b_2^0 + \frac{2!}{1!0!1!} b_0^1 b_1^0 b_2^1 + \frac{2!}{0!2!0!} b_0^0 b_1^2 b_2^0 + \frac{2!}{0!1!1!} b_0^0 b_1^1 b_2^1 + \frac{2!}{0!0!2!} b_0^0 b_1^0 b_2^2 \\
&= b_0^2 + 2b_0 b_1 + 2b_0 b_2 + b_1^2 + 2b_1 b_2 + b_2^2.
\end{aligned}$$

□

The *basis function* $B_\kappa^d(b)$ of the multivariate spline can now be defined as follows:

$$B_\kappa^d(b) := \frac{d!}{\kappa!} b^\kappa. \tag{14}$$

De Boor proved[27] that $\left\{ B_\kappa^d(b),\ \kappa \in \mathbb{N}^{n+1},\ |\kappa| = d \right\}$ is a stable basis for the space of polynomials of degree d. This means that any polynomial $p(b)$ of degree d can be written as a linear combination of B_κ^d. This linear combination of basis function is the B-form, which has the following notation:

$$p(b) = \sum_{|\kappa|=d} c_\kappa B_\kappa^d(b), \tag{15}$$

with c_κ a vector of linear coefficients called control coefficients, or more commonly, *B-coefficients*. The subscript multi-index κ is alternatively called the *indexer* of c. The total number of B-coefficients for a d-th order basis function on an n-dimensional simplex is equal to the total number of valid permutations of κ: $\hat{d}$, with $\hat{d}$ given by Eq. (12). The B-form can be evaluated using with the *de Casteljau* algorithm from,[26] or directly by simply expanding the B-form Eq. (15), which is computationally more efficient.

E. The B-coefficient net

The B-coefficients are strongly structured in what is called the B-coefficient net, or *B-net* for short. The B-net has a spatial representation that provides insight into the structure of the B-form. The B-net is also very useful in the visualization of the structure of continuity between simplices. The graphical representation of the B-net is well known in the literature, see e.g.[28, 29, 22] In Fig. 4 the graphical representation of the B-net corresponding with a third degree basis function (i.e. $d = 3$) defined on a triangulation consisting of the three simplices t_i, t_j and t_k is shown. There exists a direct relationship between the index of a B-coefficient and its spatial location, or barycentric coordinate within a simplex:

$$b(c_\kappa) = \frac{\kappa_0 v_{p_0} + \kappa_1 v_{p_1} + \cdots + \kappa_n v_{p_n}}{d}, \quad |\kappa| = d \tag{16}$$

with $b(c_\kappa)$ the barycentric coordinate of B-coefficients and $v_{p_i}, i = 0, 1, \ldots, n$ the simplex vertices.

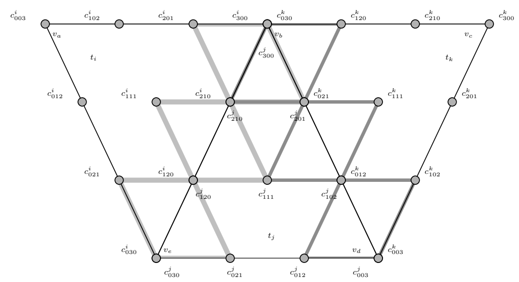

Fig. 4 B-net for $d = 3$ basis function on 3 simplices together with C^1 continuity structure

The graphical interpretation of the B-net has many uses in multivariate simplex spline theory. In this paper, the B-net plays an important role in the definition of the variance and CRLB hyper-surfaces.

F. Continuity between Simplices

A spline function is a piecewise defined polynomial function with C^r continuity between its pieces. Continuity between the polynomial pieces is enforced by continuity conditions which are defined for every facet shared by two neighboring simplices. The formulation of the continuity conditions in this subsection are well known in the literature see e.g.[27, 30, 22, 18] We use the formulation for the continuity conditions from Awanou[16] and Lai:[22]

$$c^{t_i}_{(\kappa_0,\ldots,\kappa_{n-1},m)} = \sum_{|\gamma|=m} c^{t_j}_{(\kappa_0,\ldots,\kappa_{n-1},0)+\gamma} B^m_\gamma(\sigma), \quad 0 \leq m \leq r, \tag{17}$$

with $\gamma = (\gamma_0, \gamma_1, \ldots, \gamma_n)$ a multi-index independent of κ and t_i and t_j neighboring simplices. Eventually we want all continuity conditions for all facets formulated in the following matrix form:

$$\mathbf{H}\mathbf{c} = 0, \tag{18}$$

with matrix $\mathbf{H}$ the so-called smoothness matrix and $\mathbf{c}$ the global vector of B-coefficients defined as follows:

$$\mathbf{c} = \begin{bmatrix} \mathbf{c}^{t_1} & \mathbf{c}^{t_2} & \cdots & \mathbf{c}^{t_J}, \end{bmatrix} \tag{19}$$

with $\mathbf{c}^{t_i}$ the lexicographically sorted vectors of per-simplex B-coefficients, see.[18]

In[18] an example was given for the construction of $\mathbf{H}$. It was also shown that, in general, $\mathbf{H}$ is not of full rank. For the purposes of system identification with simplex splines, however, we require $\mathbf{H}$ to be of full rank. The simplest way to achieve a full rank smoothness matrix is to reduce $\mathbf{H}$ into a row-reduced echelon form, and then truncate the resulting matrix so as to exclude all rows containing only zeros.

G. Estimating B-coefficients

The B-coefficients from Eq. (15) completely determine the shape of the spline model. In[18] a least squares method for estimating the B-coefficients of simplex splines was presented. It was shown that the estimation problem can be formulated as a Karush-Kuhn-Tucker (KKT) system as follows:

$$\begin{bmatrix} \mathbf{X}^\top \mathbf{X} & \mathbf{H}^\top \\ \mathbf{H} & 0 \end{bmatrix} \begin{bmatrix} \mathbf{c} \\ \nu \end{bmatrix} = \begin{bmatrix} \mathbf{X}^\top \mathbf{Y} \\ 0 \end{bmatrix} \tag{20}$$

with $\mathbf{X}$ the regression matrix of B-form polynomials, $\mathbf{H}$ the smoothness matrix from Eq. (18), $\mathbf{c}$ the array of all B-coefficients for the complete triangulation and with ν a set of Lagrange multipliers. The system Eq. (20) can then be solved either directly[18] or iteratively.[16]

III. System Identification with Simplex Splines

In this section a brief introduction on system identification with simplex splines is be given. The linear regression scheme presented in this section is from[18] where it was first introduced.

A. Preliminaries on linear regression with simplex splines

Consider the pair of observations $(x(i), y(i))$ related as follows:

$$y(i) = f(x(i)) + r(i), \quad i = 1, 2, \ldots, N, \tag{21}$$

with f an unknown function and with $r(i)$ a residual term. In[18] a linear regression model structure for approximating f with B-form polynomials is presented. This model structure is equivalent to a linear combination of B-form polynomials in $\mathbf{b}(i)$, with $\mathbf{b}(i)$ the barycentric coordinate of $\mathbf{x}(i)$ with respect to the simplex t_j as in Eq. (3). The B-form polynomials are of degree d and defined on a triangulation consisting of J simplices:

$$y(i) = \sum_{j=1}^{J} \left(\delta_{jk(i)} \sum_{|\kappa|=d} c_\kappa^{t_j} B_\kappa^d(b(i)) \right) + r(i), \tag{22}$$

with $\delta_{jk(i)}$ the simplex membership operator defined as follows:

$$\delta_{jk(i)} = \begin{cases} 1, & \text{if } j = k(i) \\ 0, & \text{if } j \neq k(i) \end{cases}, \tag{23}$$

and with $k(i)$ an index function that produces the index of the simplex which contains the data point $x(i)$, i.e., $x(i) \in t_{k(i)}, \ \forall i$.

□ **Example:** Define the regression model as a first degree multivariate spline function defined on two triangles. In this case the dimension $n = 2$, which leads to the following model structure:

$$\begin{aligned} y(i) &= \sum_{|\kappa|=1} c_\kappa^{t_1} B_\kappa^1(b(i)) + \sum_{|\kappa|=1} c_\kappa^{t_2} B_\kappa^1(b(i)) + \epsilon(i) \\ &= c_{100}^{t_1} b_0(i) + c_{010}^{t_1} b_1(i) + c_{001}^{t_1} b_2(i) + c_{100}^{t_2} b_0(i) + c_{010}^{t_2} b_1(i) + c_{001}^{t_2} b_2(i) + \epsilon(i) \end{aligned}$$

□

In[18] a matrix formulation of the B-form for a triangulation consisting of J simplices was presented. It was shown that a data-membership matrix operator must be defined to ensure that the matrix formulation is valid for the complete triangulation. For a single observation on the complete triangulation, this matrix operator was defined as follows:

$$\mathbf{D}(i) = \left[\left(\mathbf{D}_{t_j}(i) \right)_{j,j} \right]_{j=1}^{J} \in \mathbf{R}^{(J \cdot \hat{d}) \times (J \cdot \hat{d})} \tag{24}$$

in which the sub blocks $\mathbf{D}_{t_j}(i)$, located on the main diagonal of $\mathbf{D}(i)$, are defined as follows:

$$\mathbf{D}_{t_j}(i) = \left[(\delta_{j,k(i)})_{q,q} \right]_{q=1}^{\hat{d}} \in \mathbf{R}^{\hat{d} \times \hat{d}} \tag{25}$$

with $\delta_{j,k(i)}$ the membership operator from Eq. (23). The full-triangulation basis function vector for a single observation is found using Eq. (27):

$$\mathbf{B}^d(i) = [\ \mathbf{B}^d_{t_1}(i) \quad \mathbf{B}^d_{t_2}(i) \quad \cdots \quad \mathbf{B}^d_{t_J}(i)\ ] \ \in \mathbf{R}^{1\times J\cdot\hat{d}} \tag{26}$$

with $\mathbf{B}^d_{t_j}(i)$ the individual, lexicographically sorted basis function terms from Eq. (14):

$$\mathbf{B}^d_{t_j}(i) = [B^{d,t_j}_{\kappa}(b(i))]_{|\kappa|=d} \ \in \mathbf{R}^{1\times\hat{d}} \tag{27}$$

The B-form of the multivariate simplex spline for the complete triangulation is the result of combining Eq. (19), Eq. (26) and Eq. (24):

$$p(b(i)) = \mathbf{B}^d(i)\cdot\mathbf{D}(i)\cdot\mathbf{c} \ \in \mathbf{R}^{1\times 1} \tag{28}$$

Now let $\mathbf{X}(i)$ be a single row in the full-triangulation regression matrix for all observations $\mathbf{X} \ \in \mathbf{R}^{N\times J\cdot\hat{d}}$ as follows:

$$\mathbf{X}(i) = \mathbf{B}^d(i)\cdot\mathbf{D}(i) \ \in \mathbf{R}^{1\times J\cdot\hat{d}} \tag{29}$$

Returning to the linear regression model from Eq. (22), we then have for a single observation $y(i)$:

$$y(i) = \mathbf{X}(i)\mathbf{c} + r(i) \ \in \mathbf{R}^{1\times 1} \tag{30}$$

which, for all observations, leads to the well known formulation:

$$\mathbf{y} = \mathbf{Xc} + \mathbf{r} \ \in \mathbf{R}^{N\times 1} \tag{31}$$

B. A least squares estimator for the B-coefficients

Equation Eq. (31) can be solved using many different methods, depending on the assumptions made on the nature of the residual term $\mathbf{r}$. We will introduce a least squares (LS) estimator for Eq. (31), which implies the following assumptions on the residual $\mathbf{r}$:

$$E(\mathbf{r}) = 0, \quad Cov(\mathbf{r}) = \sigma \tag{32}$$

The well known LS cost function is:

$$J_{LS}(\mathbf{c}) = \frac{1}{2}(\mathbf{Y}-\mathbf{Xc})^\top(\mathbf{Y}-\mathbf{Xc}) \tag{33}$$

Up to this point we have not discussed how continuity between simplices is achieved in the frame of the new regression scheme. As explained in Section F, the continuity conditions are contained in the smoothness matrix $\mathbf{H}$ from Eq. (18). The continuity conditions act as constraints on B-coefficients located in the continuity structure of a triangulation. Therefore, the complete optimization problem can be stated as an equality constrained GLS problem (ECGLS) as follows:

$$\min_{\mathbf{c}} \ J_{LS}(\mathbf{c}), \text{ subject to } \mathbf{Hc} = 0 \tag{34}$$

Using Lagrange multipliers this optimization problem can be formulated as a Karush-Kuhn-Tucker (KKT) system:

$$\begin{bmatrix} \mathbf{X}^\top\mathbf{X} & \mathbf{H}^\top \\ \mathbf{H} & 0 \end{bmatrix}\begin{bmatrix} \mathbf{c} \\ \nu \end{bmatrix} = \begin{bmatrix} \mathbf{X}^\top\mathbf{Y} \\ 0 \end{bmatrix} \tag{35}$$

with ν vector of Lagrange multipliers. The coefficient matrix in Eq. (35) is the KKT matrix. The solution of the KKT system is:

$$\begin{bmatrix} \hat{\mathbf{c}} \\ \hat{\nu} \end{bmatrix} = \begin{bmatrix} \mathbf{C_1} & \mathbf{C_2} \\ \mathbf{C_3} & \mathbf{C_4} \end{bmatrix}\cdot\begin{bmatrix} \mathbf{X}^\top\mathbf{Y} \\ 0 \end{bmatrix} \tag{36}$$

with $\hat{\mathbf{c}}$ and $\hat{\nu}$ estimators for $\mathbf{c}$ and ν respectively. Rao shows in[31] that the matrix in Eq. (36) is equal to the inverse of the KKT matrix:

$$\begin{bmatrix} \mathbf{C_1} & \mathbf{C_2} \\ \mathbf{C_3} & \mathbf{C_4} \end{bmatrix} = \begin{bmatrix} \mathbf{X}^\top\mathbf{X} & \mathbf{H}^\top \\ \mathbf{H} & 0 \end{bmatrix}^{-1} \tag{37}$$

Note that the sizes of the submatrices $\mathbf{C_1}$, $\mathbf{C_2}$ and $\mathbf{C_3}$ in Eq. (37) are equal to the sizes of $\mathbf{X}^\top\mathbf{X}$, $\mathbf{H}^\top$ and $\mathbf{H}$ respectively.

IV. Aerodynamic Model Validation

In this section the multivariate simplex spline based model for the aerodynamic pitching moment coefficient of the Cessna Citation II is validated. This model was identified using flight data collected during 76 longitudinal 3211 flight test maneuvers.[21] Flight path reconstruction techniques based on an iterated extended Kalman filter (IEKF) were used to get a crisp estimation of aircraft state.[32] The linear regression scheme for multivariate simplex splines from Sec. II was then used with the reconstructed aircraft state to identify a simplex spline based model for the non-dimensional aerodynamic pitching moment coefficient C_m.

The new model validation method was then used to assess the quality of the created spline model. Two different analysis methods were used: the first method is a model residual analysis, and the second method is a statistical analysis of the parameters of the multivariate splines. It will be shown that both validation methods complement each other and together provide an extremely powerful method for assessing the quality of an aerodynamic model.

A. Aerodynamic model identification with multivariate splines

Using the theory from Sec. II and Sec. III a multivariate simplex based model for the pitching moment coefficient C_m was identified. The data for aerodynamic model identification was collected during 76 longitudinal 3211 flight test manoeuvres. The manoeuvres where executed between 5000 and 5500 meters, with airspeed ranging from 90 m/s till 170 m/s while the thrust setting was kept constant. The aircraft was in a clean configuration during all manoeuvres. The flight path reconstruction technique from Mulder et al.[32] was used to derive crisp aircraft states from the measurement data. The crisp aircraft states where used to calculate the aerodynamic pitching moment coefficient C_m as follows (see e.g. Stevens and Lewis[33]):

$$C_m = \frac{1}{\frac{1}{2}\rho V^2 S\bar{c}}\big(I_y\dot{q} - (I_z - I_x)rp - I_{xz}(r^2 - p^2)\big), \tag{38}$$

$$\tag{39}$$

with p, q and r the angular rates about the F_B. I_x, I_y, and I_z are the products of inertia, while I_{xz} is the single non-zero cross-product of inertia.

The following model structure was used for the aerodynamic model for C_m:

$$C_m = f_m(\alpha, q, \delta_e) \in S_3^1(\mathcal{T}) \tag{40}$$

with $f_m(\alpha, q, \delta_e)$ a trivariate spline function of the angle of attack α, the pitch rate q and the elevator deflection δ_e. The spline function is a member of the spline space $S_3^1(\mathcal{T})$ which is of degree 3 with C^1 continuity on the triangulation $\mathcal{T}$ which in this case consisted of 18 simplices (tetrahedrons), see Fig. 5. This particular model structure was chosen because it was the simplest model structure to produce adequate results.

The multivariate simplex spline model was identified with a least squares estimator which used a subset of the complete dataset as identification dataset. The model output from the spline function $f_m(\alpha, q, \delta_e)$ modeling the pitching moment coefficient C_m is shown in Fig. 6. The model of C_m shows some interesting facts. First, it is clear that C_m is highly nonlinear along all model dimensions. Second, the slope of the model for C_m in the direction of α is observed to be positive at some flight conditions, that is, $C_{m_\alpha} > 0$. This is somewhat unexpected for a statically stable aircraft like the Cessna Citation II. In Table 1 the numerical results from the experiment are presented.

B. Validating the multivariate simplex spline based aerodynamic model

The multivariate spline based aerodynamic model was validated using two different methods. First, a model residual analysis was performed in which the local model error was itself modeled with a secondary simplex spline function. Second, an analysis of the estimated variances in the B-coefficients of the multivariate simplex splines was performed. The data used to validate the model was a subset of the complete dataset which was completely independent of the identification dataset.

Starting with the model residual analysis, we define the model residual as follows:

$$\epsilon_m(\alpha, q, \delta_e) := f_m(\alpha, q, \delta_e) - C_m. \tag{41}$$

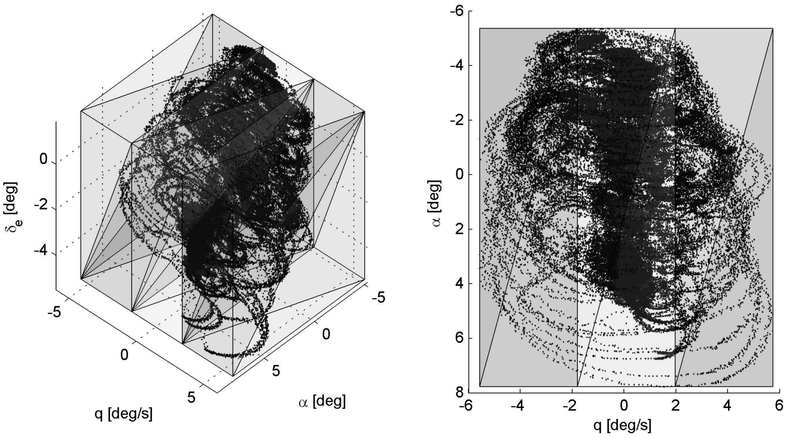

Fig. 5 The triangulation consisting of 18 tetrahedrons together with the dataset used for aerodynamic model identification.

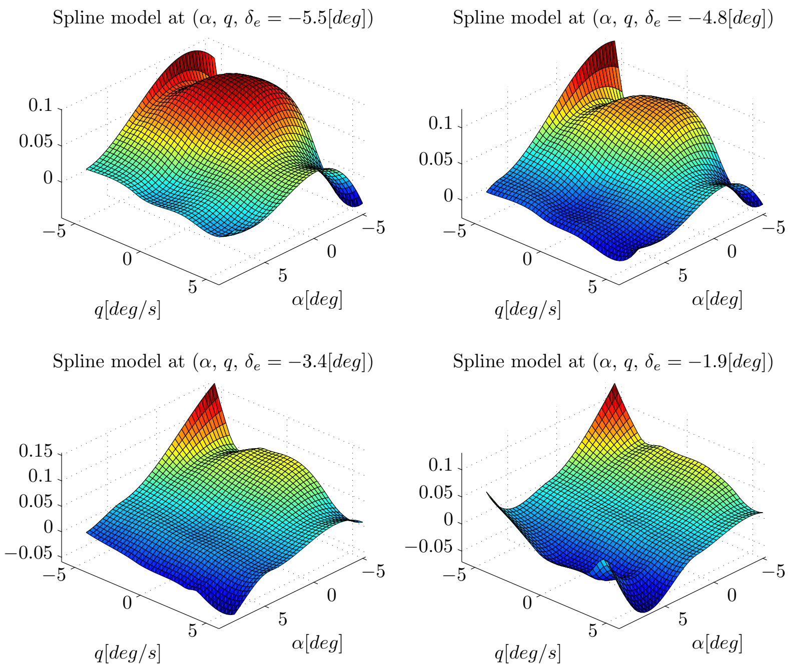

Fig. 6 Four 3-D slices through the global spline model $f_m(\alpha, q, \delta_e)$ for C_m along the δ_e axis

with C_m the measured aerodynamic pitching moment coefficient from Eq. (39).

The model residual is calculated using the validation dataset, which is unrelated to the identification dataset used to identify f_m. In Fig. 7 the measured output for C_m together with the spline output f_m and the model residual ϵ_m from Eq. (41) is plotted. Global numerical results from the model validation are shown in Table 1.

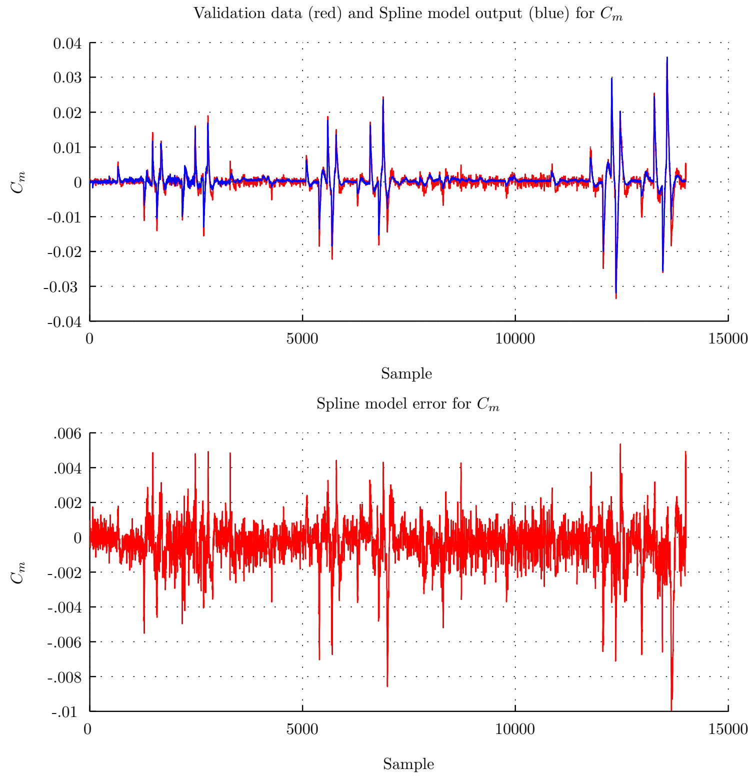

Fig. 7 Comparison between measured values for C_m and model output from $f_m(\alpha, q, \delta_e)$ (top) and the model residual ϵ_m (bottom).

Table 1 Results of the model validation

Spline model	Simplices	error RMS	relative error RMS
$f_m(\alpha, q, \delta_e) \in S_3^1(\mathcal{T}_m)$	18	1.84e-003	1.72%

Using Chebychev's inequality, confidence bounds were calculated for the residual of the spline model. Chebychev's inequality states that any set of data, no matter its distribution, is more than k standard deviations away from its mean. More precisely, if μ is the mean of ϵ_m and σ is its standard deviation, then Chebychev's inequality is:

$$P(|\epsilon_m - \mu| \geq k\sigma) \leq \frac{1}{k^2} \tag{42}$$

It is important to note that the confidence bounds calculated using Chebychev's inequality are more conservative than bounds calculated based on the normal distribution. Using $k = 4$ in Eq. (42), 94% of the model residual should be within the confidence bounds. Instead of calculating global confidence bounds, the complete model was partitioned into 1300 subregions, each containing sufficient data to allow the use of Chebychev's inequality. After the partitioning, confidence bounds were calculated for each subregion. These local confidence bounds then contained at 94% of the local model residual. A new multivariate simplex spline function of the same degree as f_m was then used to blend the local confidence bounds together into a new global confidence bound model f_{bound}.

The resulting 4σ confidence bound model f_{bound} is shown in Fig. 8. The confidence bound model clearly shows that the quality of the spline model at the edges of the model domain is of lower quality than in the interior regions. Especially the regions in the model domain for which $q < -4$ and $q > 4$ have significantly wider 4σ confidence bounds than interior model regions.

Following the model residual analysis, a statistical model quality analysis was performed. This quality analysis uses the estimated covariances of the B-coefficients to create a variance hyper-surface. It was found in[18] that the B-coefficient covariance matrix is given by:

$$Cov(\hat{c}) = \text{diag}(\mathbf{C_1}), \tag{43}$$

with $\mathbf{C_1}$ the upper left block of the Fisher Information Matrix from Eq. (37). From Eq. (43) the variance of the B-coefficients can be found as follows:

$$Var(\hat{c}) = \text{diag}(\mathbf{C_1}), \tag{44}$$

The Cramér-Rao Lower Bound (CRLB) of the B-coefficients is then given by:

$$CRLB(\hat{c}) \geq Var(\hat{c}), \tag{45}$$

The CRLB of the B-coefficients can now be used to define a special hyper-surface containing the B-coefficient CRLB's. This is possible because the B-coefficients have a unique spatial location within a simplex. A B-coefficient variance, or CRLB, can therefore be directly translated to a spatial location. In Fig. 9 the B-coefficient CRLB surface of the spline model f_m is shown. The CRLB surface clearly shows that there are two model regions in which the B-coefficient CRLB is extremely high; the region ($\alpha < -2$ $[deg], q < -3$ $[deg/s]$) and the region ($\alpha > 4$ $[deg], q > 4$ $[deg/s]$). These regions correspond to parts of the flight envelope which contain little to no flight data, see Fig. 5. The variance surface can also point to areas in the model in which the identification has a high noise content

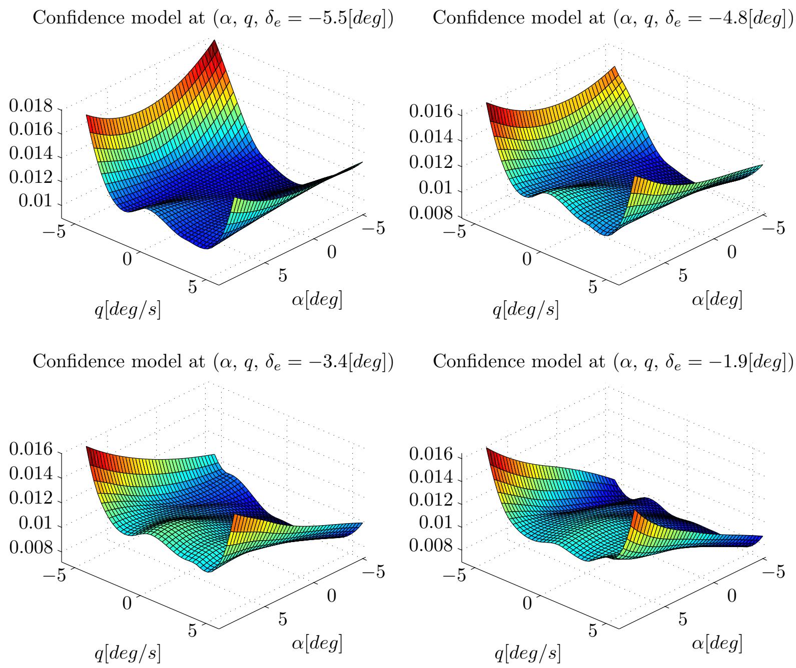

Fig. 8   Four 3-D slices through the 4σ spline confidence model $f_{bound}(\alpha, q, \delta_e)$ for C_m along the δ_e axis.

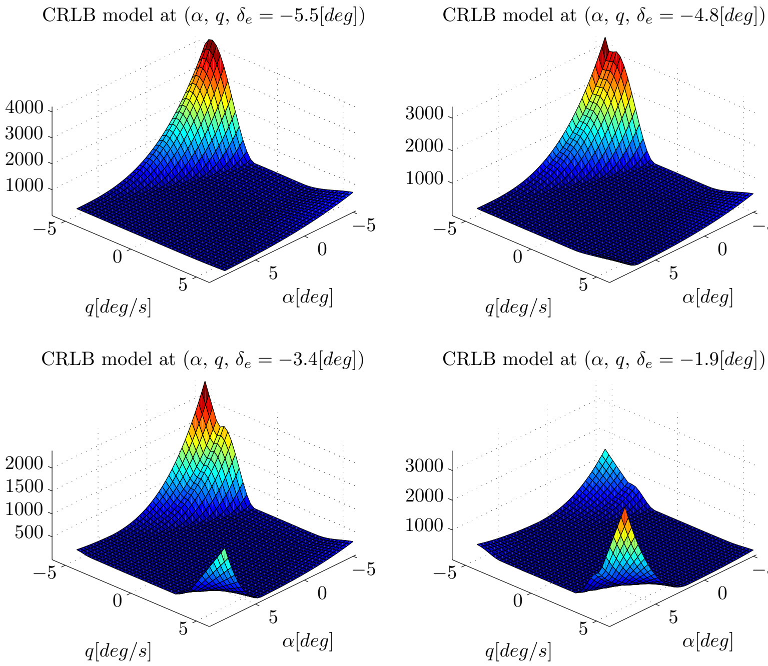

Fig. 9 Four 3-D slices through the parameter CRLB model $f_m(\alpha, q, \delta_e)$ for C_m along the δ_e axis

V. Conclusion

In this paper, a global nonlinear aerodynamic model of the Cessna Citation II laboratory aircraft is validated using two new model validation approaches. These new model validation approaches are made possible by a new method for aerodynamic model identification based on multivariate simplex splines. The multivariate simplex splines have a number of unique properties, such as the ability to fit scattered multi-dimensional data on non-rectangular domains, and the fact that the parameters of the simplex splines have a unique spatial location within the spline model.

The first new validation approach is a model residual analysis which results in a secondary simplex spline function for the confidence bounds of the aerodynamic model. The second new approach is a statistical model quality analysis which produces a parameter variance surface in which the variance of each individual model parameter has a unique spatial location within the model domain. The parameter variance surface then allows the pinpointing of regions of high parameter variance within the aerodynamic model.

The new model validation approaches were demonstrated by validating a multivariate simplex spline based model for the aerodynamic pitching moment coefficient of the Cessna Citation II. This model was identified using a set of 5 million data points collected during 76 longitudinal flight test maneuvers. The statistical model quality analysis showed that the quality of the multivariate spline based model was high except for parts of the flight envelope in which data was scarce.

Together, the two new model validation approaches provide a powerful new method of assessing the quality of an aerodynamic model based on multivariate simplex splines. The two new model quality measures in the form of the confidence bound spline model and the parameter variance surface can be used to efficiently and accurately pinpoint regions within the aerodynamic model which require more or higher quality flight data.

References

[1]Iliff, K. W., Maine, R., and Montgomery, T., "Important Factors in the Maximum Likelihood Analysis of Flight Test Maneuvers," Tecnical Paper 1459, NASA, 1979.

[2]Klein, V., Batterson, J. G., and Murphy, P. C., "Determination Of Aircraft Model Structure From Flight Data By Using Modified Stepwise Regression," Tech. Rep. 1916, NASA, 1981.

[3]Mulder, J. A., *Design and Evaluation of Dynamic Flight Test Maneuvers*, Ph.D. thesis, Delft University of Technology, 1986.

[4]Klein, V., "Estimation of Aircraft Aerodynamic Parameters from Flight Data," *Progress in Aerospace Sciences*, Vol. 26, 1989, pp. 1–77.

[5]Morelli, E. A., "Global Nonlinear Aerodynamic Modeling Using Multivariate Orthogonal Functions," *AIAA Journal of Aircraft*, Vol. 32, 1995, pp. 270–277.

[6]Morelli, E. A., "Global Nonlinear Parameteric Modeling with Application to F-16 Aerodynamics," *American Control Conference*, 1998.

[7]Morelli, E. A. and Klein, V., "Accuracy of Aerodynamic Model Parameters Estimated From Flight Test Data," *Journal of Guidance Control and Dynamics*, Vol. 20, 1997, pp. 74–80.

[8]Klein, V. and Morelli, E. A., *Aircraft System Identification*, AIAA, 2006.

[9]Jategaonkar, R. V., *Flight Vehicle System Identification*, Vol. 216 of *Progress in Astronautics and Aeronautics*, AIAA, 2006.

[10]Lombaerts, T. J. J., Chu, Q. P., Mulder, J. A., and Joosten, D. A., "Real Time Damaged Aircraft Model Identification for Reconfiguring Flight Control," *AIAA Atmospheric Flight Mechanics Conference and Exhibit*, 2007.

[11]Smith, P. L., "Curve Fitting and Modeling with Splines Using Statistical Variable Selection Techniques," Contractor Report NASA-CR-166034, NASA, 1982.

[12]Bruce, P. D. and Kellett, M. G., "Modelling and identification of non-linear aerodynamic functions using B-splines," *Proceedings of the Institution of Mechanical Engineers, Part G: Journal of Aerospace Engineering*, Vol. 214, 2000, pp. 27–40.

[13]Dahmen, W., Micchelli, C. A., and Seidel, H. P., "Blossoming Begets B-Spline Bases Built Better By B-Patches," *Mathematics of Compuatation*, Vol. 59, 1992, pp. 97–115.

[14]Forrest, A. R., "Interactive Interpolation and Approximation by Bézier Polynomials," *Computer Aided Design*, Vol. 22, No. 9, 1990, pp. 527–537, Reprint of The Computer Journal, 15(1):71-79, 1972.

[15]Anderson, I. J., Cox, M. G., and Mason, J. C., "Tensor-Product Spline Interpolation to Data On or Near a Family of Lines," *Numerical Algorithms*, Vol. 5, 1993, pp. 193–204.

[16]Awanou, G., Lai, M. J., and Wenston, P., "The Multivariate Spline Method for Scattered Data Fitting and Numerical Solutions of Partial Differential Equations," *Wavelets and Splines*, edited by G. Chen and M. J. Lai, 2005, pp. 24–75.

[17]Lai, M. J., "Multivariate Splines for Data Fitting and Approximation," *12th Approximation Theory Conference*, 2007.

[18]de Visser, C. C., Chu, Q. P., and Mulder, J. A., "A New Approach to Linear Regression with Multivariate Splines," *Automatica*, Vol. 45, No. 12, 2009, pp. 2903–2909.

[19]Lombaerts, T. J. J., Oort, E. R. V., Chu, Q. P., Mulder, J. A., and Joosten, D. A., "Online Aerodynamic Model Structure Selection and Parameter Estimation for Fault-Tolerant Control," *Journal Of Guidance, Control, and Dynamics*, Vol. 33, 2010, pp. 707.

[20]de Visser, C., Mulder, J., and Chu, Q., "Global Nonlinear Aerodynamic Model Identification with Multivariate Splines," *AIAA Atmospheric Flight Mechanics Conference*, 2009.

[21]de Visser, C., Mulder, J. A., and Chu, Q. P., "A Multidimensional Spline Based Global Nonlinear Aerodynamic Model for the Cessna Citation II," *AIAA Atmospheric Flight Mechanics Conference*, 2010.

[22]Lai, M. J. and Schumaker, L. L., *Spline Functions over Triangulations*, Cambridge University Press, 2007.

[23]Ruppert, J., "A Delaunay Refinement Algorithm for Quality 2-Dimensional Mesh Generation," *Journal of Algorithms*, Vol. 18, 1995, pp. 548–585.

[24]Lai, M., "Some Sufficient Conditions For Convexity of Multivariate Bernstein-B'ezier Polynomials and Box Spline Surfaces," *Studia Scient. Math. Hung.*, Vol. 28, 1990, pp. 363–374.

[25]Lai, M. J. and Schumaker, L. L., "On the Approximation Power of Bivariate Splines," *Advances in Computational Mathematics*, Vol. 9, 1998, pp. 251–279.

[26]Hu, X. L., Han, D. F., and Lai, M. J., "Bivariate Splines of Various Degrees for Numerical Solution of Partial Differential Equations," *SIAM Journal on Scientific Computing*, Vol. 29, 2007, pp. 1338–1354.

[27]de Boor, C., "B-form Basics," *Geometric modeling: algorithms and new trends*, edited by G. Farin, SIAM, 1987.

[28]Farin, G., "Triangular Bernstein-Bézier Patches," *Computer Aided Geometric Design*, Vol. 3, 1986, pp. 83–127.

[29]Lai, M. J., "Geometric Interpretation of Smoothness Conditions of Triangular Polynomial Patches," *Computer Aided Geometric Design*, Vol. 14, 1997, pp. 191–199.

[30]Awanou, G., *Energy Methods in 3D spline approximations of the Navier-Stokes Equations*, Ph.D. thesis, University of Georgia, 2003.

[31]Rao, C. R., *Linear Statistical Inference and Its Applications*, John Wiley & Sons, Inc., 2002.

[32]Mulder, J. A., Chu, Q. P., Sridhar, J. K., Breeman, J. H., and Laban, M., "Non-Linear Aircraft Flight Path Reconstruction Review and New Advances," *Progress in Aerospace Sciences*, Vol. 35, 1999, pp. 673–726.

[33]Stevens, B. L. and Lewis, F. L., *Aircraft Control and Simulation*, John Wiley & Sons, Inc., 2003.